



A needle in a haystack: Integrative taxonomy reveals the existence of a new small species of fossorial frog (Anura, Microhylidae, *Synapturanus*) from the vast lower Putumayo basin, Peru

Germán Chávez^{1,2}, Michelle E. Thompson³, David A. Sánchez⁴, Juan Carlos Chávez-Arribasplata^{1,2}, Alessandro Catenazzi^{1,2,5}

¹ Instituto Peruano de Herpetología (IPH), Lima, Peru

² Division de Herpetología – CORBIDI, Lima, Peru

³ Keller Science Action Center, Science & Education, Field Museum of Natural History, Chicago, IL, USA

⁴ Instituto Amazónico de Investigaciones Científicas SINCHI, Bogotá, Colombia

⁵ Department of Biological Sciences, Florida International University, 11200 SW 8th St., Miami, FL 33199, USA

<http://zoobank.org/7F4C67F6-9091-4C60-9B72-6EC080517099>

Corresponding author: Germán Chávez (vampflack@yahoo.com)

Academic editor: Alexander Haas ♦ Received 8 January 2022 ♦ Accepted 7 February 2022 ♦ Published 16 February 2022

Abstract

We describe a new species of microhylid frog of the genus *Synapturanus* from the lower Putumayo basin in Loreto, Perú. Specimens inhabited the soils of stunted pole forests growing on peat. The new species is distinguished from other species of *Synapturanus* through morphology, genetics, and acoustic characteristics. This species differs from most nominal congeners by having a head flat in lateral view (vs convex in the rest of species), a characteristic only shared by *S. rabus* and *S. salseri*. The new species can be distinguished from *S. rabus* and *S. salseri* by a combination of morphological characters and by having an advertisement call with a note length of 0.05–0.06 seconds (vs 0.03 seconds in *S. rabus*) and a dominant frequency ranging from 1.73 to 1.81 kHz (vs 1.10–1.47 kHz in *S. salseri*). Principal component analyses of 12 morphological characters and three acoustic variables further support differences between the new species and its described and undescribed congeners.

Key Words

Acoustic, genetic, Loreto, morphology, peatland

Introduction

Owing to their fossorial habits, frogs of the microhylid genus *Synapturanus* have been scarcely studied and therefore, their diversity is likely underestimated. Recently Fouquet et al. (2021a, b) delved deeper into *Synapturanus* taxonomy and described three new species to recognize six taxa: *S. ajuricaba* Fouquet et al. 2021b, from eastern Amazonia, *S. mesomorphus* Fouquet et al., 2021b from the Guiana Shield, *S. mirandariberoi* Nelson & Lescure, 1975 from the Guiana Shield, *S. rabus* Pyburn, 1976 and *S. salseri* Pyburn, 1975 from the Colombian Amazonia, and *S. zombie* Fouquet et al., 2021b from

the Guiana Shield. The major center of diversity of these frogs appears to be in the Guiana Region and Eastern Amazonia. Nonetheless, it is likely that many undescribed species have already been documented and it is likely that more remain given the fossorial habits of these frogs reduce their detectability and given their limited dispersal abilities and putative narrow ranges lead to many microendemics (Fouquet et al. 2021b).

Three localities in Fouquet et al. (2021a) are within or near Peruvian territory: two sites in the vicinity of Sierra del Divisor National Park (*Synapturanus* sp. “Divisor”), a protected area shared between Perú and Brazil, south of the Amazon River, and the remaining site in the

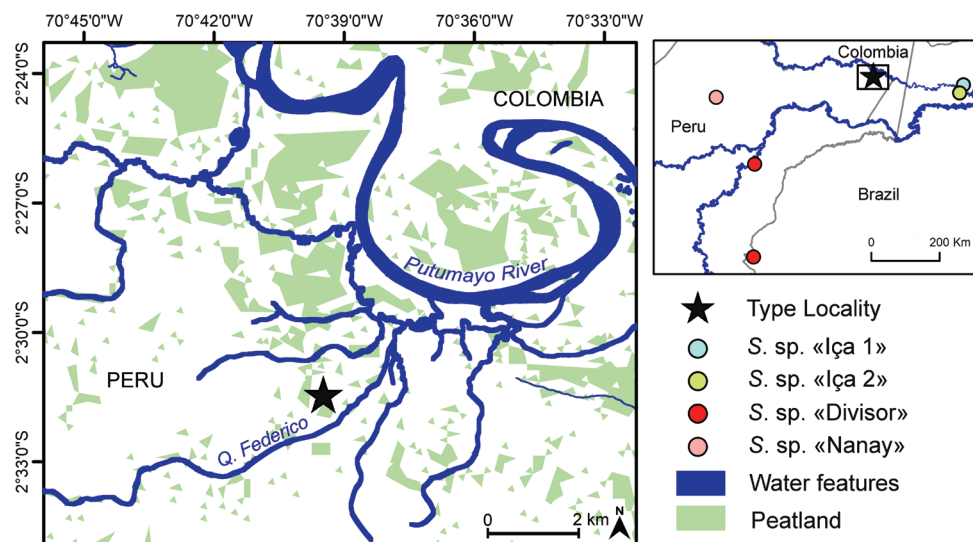


Figure 1. Map showing the type locality of *Synapturanus danta* sp. nov. (black star), and the localities of the closest populations of *Synapturanus*. Those correspond to four undescribed taxa (Fouquet et al. 2021a): *S.* sp. “Iça 1” (pale blue circle). *S.* sp. “Iça 2” (yellow circle) from Brazil, *S.* sp. “Divisor” from Brazil and Perú (red circles), and *S.* sp. “Nanay” from Perú (pink circle). Green patches represent Amazon peatlands present in the area (Xu et al. 2018).

Nanay River (*Synapturanus* sp. “Nanay”, one of the main tributaries of the Amazon River in northern Peru. Fouquet et al. (2021a) also include two candidate species (*Synapturanus* sp. “Iça 1” and *S.* sp. “Iça 2”) from Brazil, sampled on opposite sides of the Putumayo River near its junction with the Amazonas River, about 240 km airline from the nearest border of Perú (Fig. 1).

Measuring approximately 1600 km, the Putumayo River is located in a biodiversity hotspot (Pitman et al. 2021), and its basin drains vast expanses of intact forests (Jarrett et al. 2021) in Colombia, Ecuador, Perú and Brazil (Ziesler and Ardizzone 1979). The Putumayo is the last remaining Amazon tributary without existing or proposed dams (Anderson et al. 2018). The diversity of amphibians of the Putumayo basin is understudied and underestimated (Chávez et al. 2021). To help fill the knowledge gap of herpetofauna diversity, we performed an expedition as part of a Field Museum rapid biological and social inventory (Pitman et al. 2021) between 5–25 November 2019 in the lower Putumayo basin (Chávez et al. 2021), where we collected a small series of *Synapturanus*. After morphological examination, acoustic and molecular analyses, we conclude that these frogs belong to a species distinct from any other described *Synapturanus* as well as being genetically differentiable from those mentioned as candidate species by Fouquet et al. (2021a, b). Herein, we present the results of our analyses and the description of the new species.

Methods

Morphology

We measured 12 morphological variables on preserved specimens, following Kok and Kalamandeen (2008) and Fouquet et al. (2021a, 2021b): snout-vent length (SVL); head length, from the corner of the mouth to the tip of the

snout (HL); head width at the level of the angle of jaws (HW); eye to-naris distance, from the anterior edge of the eye to the center of the naris (EN); internarial distance (IN); horizontal eye diameter (ED); interorbital distance, representing the width of the underlying frontoparietal (IO); forearm length, from the proximal edge of the palmar tubercle to the outer edge of the flexed elbow (FAL); hand length, from the proximal edge of the palmar tubercle to the tip of the Finger III (HAND); crus (tibiofibular) length, from the outer edge of the flexed knee to the heel (TL); foot length, from the proximal edge of the inner metatarsal tubercle to the tip of Toe IV (FL); and thigh length, from the vent opening to the outer edge of the flexed knee (ThL). Tables 1, 2 show phenotypic features of current *Synapturanus* and morphological measurements of the type series of the new species respectively. Data for other *Synapturanus* have been taken from Nelson and Lescure 1975; Pyburn 1975, 1977, and Fouquet et al. 2021b.

To support our morphological diagnosis, we performed two Principal Component Analyses in PAST version 3.26 (Hammer et al. 2001): 1) a PCA with the original dataset presented in the supplementary material of Fouquet et al. (2021a) and measurements of the two males collected in lower Putumayo River; 2) a PCA with the residuals of regression of eleven measurements with size (Snout Vent Length was taken as proxy of size). Measurements taken by Fouquet et al. (2021a) are for males only, as are the two adult specimens collected in Perú. The juvenile collected in Perú was not included in the analyses.

Bioacoustics

We recorded calls from two individuals of the new species (CORBIDI 21050, 21051) calling from underground galleries at night (20:15 hrs). We used a Marantz PMD661MK2 digital recorder and a Sennheiser

Table 1. Phenotypic characters of the current species of *Synapturanus*.

	SVL in males (mm)	Body shape	Dorsal region of the head from a lateral view	Dorsal coloration	Canthal stripe	Advertisement call structure	Advertisement call note length range (seconds)	Advertisement call dominant frequency range (Khz)
<i>Synapturanus danta</i> sp. nov.	17.6–17.9	Slender	Flat	Dark Brown without spots	Present in juveniles	single tonal note	0.05–0.06	1.73–1.81
<i>S. ajuricaba</i>	29.3–33.2	Robust	Convex	Brown with orange spots	Present	single tonal note, 12–17 pulses	0.28–0.36	1.01–1.12
<i>S. mesomorphus</i>	22.9–26.0	Slender	Convex	Dark/pale brown with beige speckles	Present	single tonal note	0.16–0.17	1.06–1.13
<i>S. mirandariberoi</i>	26.2–30.8	Robust	Convex	Brown with orange spots	Present	single tonal note, 5–8 pulses	0.13–0.19	1.10–1.47
<i>S. rabus</i>	16.2–16.6	Slender	Flat	Dark Brown with light spots	Present	single tonal note	0.03	–
<i>S. salseri</i>	23.7–26.4	Robust	Flat	Brown with orange/gray spots	Present (uncontinuous)	single tonal note	0.07–0.09	1.31–1.57
<i>S. zombie</i>	37.0–40.6	Robust	Convex	Brown with numerous orange spots	Absent	single tonal note	0.14–0.16	1.06–1.19

Table 2. Measurement variation (mm) in the type series of *Synapturanus danta* sp. nov.

	CORBIDI 21050	CORBIDI 21051	CORBIDI 21013
Sex	Male	Male	Juvenile
SVL	18.0	17.6	7.5
HL	4.4	4.2	2.5
HW	5.6	5.6	2.6
EN	1.5	1.5	0.8
IN	1.1	1.1	0.5
ED	1.0	1.1	0.8
IO	2.3	2.4	1.3
FAL	2.8	2.9	1.3
HAND	2.8	2.5	1.5
TL	5.1	5.0	3.0
FL	7.5	7.7	3.8
ThL	6.9	7.3	2.9
HL/SVL	0.2	0.2	0.3
HW/SVL	0.3	0.3	0.4
HW/HL	1.3	1.3	1.0
ED/EN	0.7	0.7	1.0
FL/ TL	1.5	1.5	1.3
TL/ SVL	0.3	0.3	0.4
HAND/ SVL	0.2	0.1	0.2
FL/ SVL	0.4	0.4	0.5
IN/HW	0.2	0.2	0.2
EN/HL	0.3	0.4	0.3

ME64 uni-directional microphone. All recordings were performed at night between 24–26 °C, and 0.5 m distance from the call emitter (temperatures unknown inside the galleries). We followed the call-centered approach used by Fouquet et al. (2021b) and measured four variables (as defined by Kohler et al. 2017): Note Length (NL), Dominant Frequency (DoF, which also corresponds to the fundamental frequency in the genus; taken with a spectral slice over the entire note), Delta Frequency (DeF) (difference in peak frequency between spectral slices taken over the first and the last 0.015 seconds of the note), Inter-note length (the silence between the end of

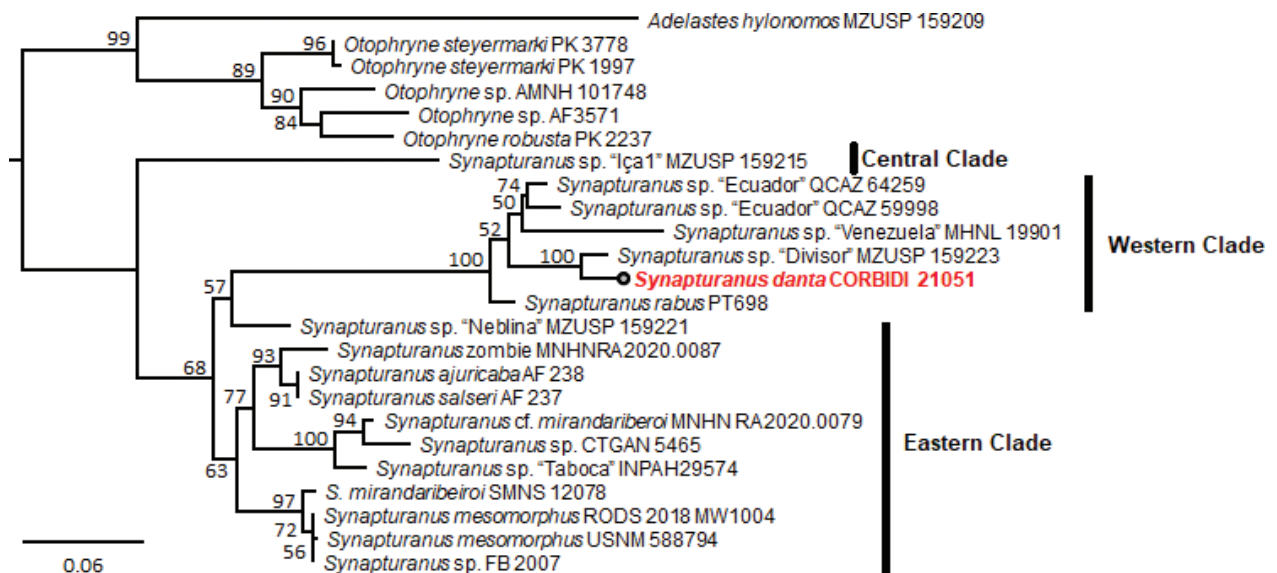
one note and the beginning of the next one). We measured call variables using package warbleR (Araya-Salas and Smith-Vidaurre 2017) and visualized spectrograms using package seewave (Sueur et al. 2008) in R v4.1.0 (R Core Team 2021). We used the average calculated across four calls of each of the two males recorded. Call parameters of the new species and congeners are summarized in Table 3. Also, we performed a PCA with three of the call variables: NL, DoF, and DeF.

Genetic analysis

We used molecular phylogenetic analyses to confirm the generic placement of the new species within *Synapturanus* (Fig. 2). We used a fragment of the mitochondrial 16S rRNA fragment, because 16S is the most frequently sequenced gene among species of *Synapturanus* (Fouquet et al. 2021a). For the new species (a single novel DNA sequence, GenBank code [OM488910](#)), we used liver tissues from CORBIDI 21051, and used a commercial extraction kit (IBI Scientific, Peosta, USA) to extract DNA. We downloaded 16S DNA sequences from of all sampled species of *Synapturanus*, as well as the closely related genera *Adelastes* and *Otophryne* (Fouquet et al. 2021a) from GenBank (Suppl. material 1: Appendix 1). Our analysis included 24 terminals. We used the 16Sar forward (5'-3' sequence: CGCCTGTTTATCAAAAACAT) and 16Sbr reverse (5'-3' sequence: CCGGTCTGAACTCAGATCACGT) primers to sequence a fragment of 16S up to 583 bp-long. The thermocycling conditions during the polymerase chain reaction (PCR) using a Proflex thermal cycler (Applied Biosystems) were: one cycle at 96 °C/3 min; 35 cycles at 95 °C/30 s, 55 °C/45 s, 72 °C/1.5 min; and one cycle at 72 °C/7 min. We purified PCR products with Exosap-IT (ThermoFisher), and shipped purified samples to MCLAB for sequencing (South San Francisco, CA, USA).

Table 3. Acoustic variables: Note length (NL), Dominant Frequency (DoL), Delta Frequency (DeF), Pulses, Internote length (Internote). Values show mean with range in parentheses. Data for other *Synapturanus* from Fouquet et al. (2021b).

Species	Sample size	NL (seconds)	DoF (Hz)	Pulses	Def (Hz)	Internote
<i>Synapturanus danta</i> sp. nov.	n=2	0.059 (0.054–0.063)	1.763 (1.734–1.809)	1 (1–1)	59 (0–94)	4.083 (3.777–4.552)
<i>S. ajuricaba</i>	n=5	0.322 (0.282–0.366)	1.064 (1.013–1.121)	14 (12–16)	57 (11–87)	6.91 (5.20–9.04)
<i>S. mesomorphus</i>	n=2	0.167 (0.160–0.173)	1.093 (1.058–1.127)	1 (1–1)	28 (15–40)	10.30 (9.66–10.93)
<i>S. mirandariberoi</i>	n=9	0.167 (0.130–0.194)	1.251 (1.100–1.471)	7 (5–8)	148 (22–256)	6.57 (4.10–11.56)
<i>S. rabus</i>	n=1	0.039	1.642	1	169	11.20
<i>S. salseri</i>	n=6	0.079 (0.071–0.090)	1.411 (1.312–1.574)	1 (1–1)	49 (14–91)	5.31 (2.36–9.16)
<i>S. zombie</i>	n=4	0.154 (0.147–0.167)	1.107 (1.059–1.190)	1 (1–1)	142 (104–194)	8.48 (6.90–9.90)

**Figure 2.** Phylogenetic analysis based on a fragment of 16S, showing the relationship among *Synapturanus danta* sp. nov. (in red), its congeners, and species of *Adelestes* and *Otophryne* (Microhylidae). ML bootstrap values are indicated at each node. Taxa assignment to central, eastern and western clade follows Fouquet et al. (2021a).

We used Geneious, version 11.1.5 (Biomatters, <http://www.geneious.com/>) to align sequences with the MAFFT v7.017 alignment program (Katoh and Standley 2013), and trimmed sequences to a length of up to 583 bp. We used PartitionFinder, v. 1.1.1 to select the best substitution model using the Bayesian information criterion (BIC). The best model was GTR + I + G. We assessed node support using 10,000 bootstrap replicates. We inferred phylogenetic relationships with Maximum Likelihood (ML) inference. We conducted the analysis with IQ-TREE v1.6.12 (Nguyen et al. 2015) using the substitution models determined by PartitionFinder, and the ultrafast bootstrap method (10000 bootstrap alignments).

We also estimated genetic distances for the 16S rRNA mitochondrial fragment to provide further support of species delimitation. Fouquet et al. (2007) suggested that 3% distance for 16S is a reasonable criterion to identify putative new species. We estimated mean uncorrected p-distances for 16S rRNA between the new species and other species of *Synapturanus*, *Otophryne* and *Adelestes* (i.e., the proportion of nucleotide sites at which any two sequences are different) with the R package “ape” (Paradis et al. 2004), and uploaded the table to Figshare (<https://doi.org/10.6084/m9.figshare.17702231>).

Nomenclatural act

The electronic version of this article in Portable Document Format (PDF) will represent a published work according to the International Commission on Zoological Nomenclature (ICZ), and hence the new name contained in the electronic version is effectively published under that Code from the electronic edition alone. This published work and the nomenclatural acts it contains have been registered in ZooBank, the online registration system for the ICZN. The ZooBank LSIDs (Life Science Identifiers) can be resolved and the associated information viewed through any standard web browser by appending the LSID to the prefix <http://zoobank.org/>. The LSID for this publication is: urn:lsid:zoobank.org:pub: 7F4C67F6-9091-4C60-9B72-6EC080517099.

Results

Generic placement

General appearance, morphological and bioacoustic characteristics, as well as our phylogenetic analyses support the placement of the new species within *Synapturanus*. According to our phylogeny (Fig. 2),

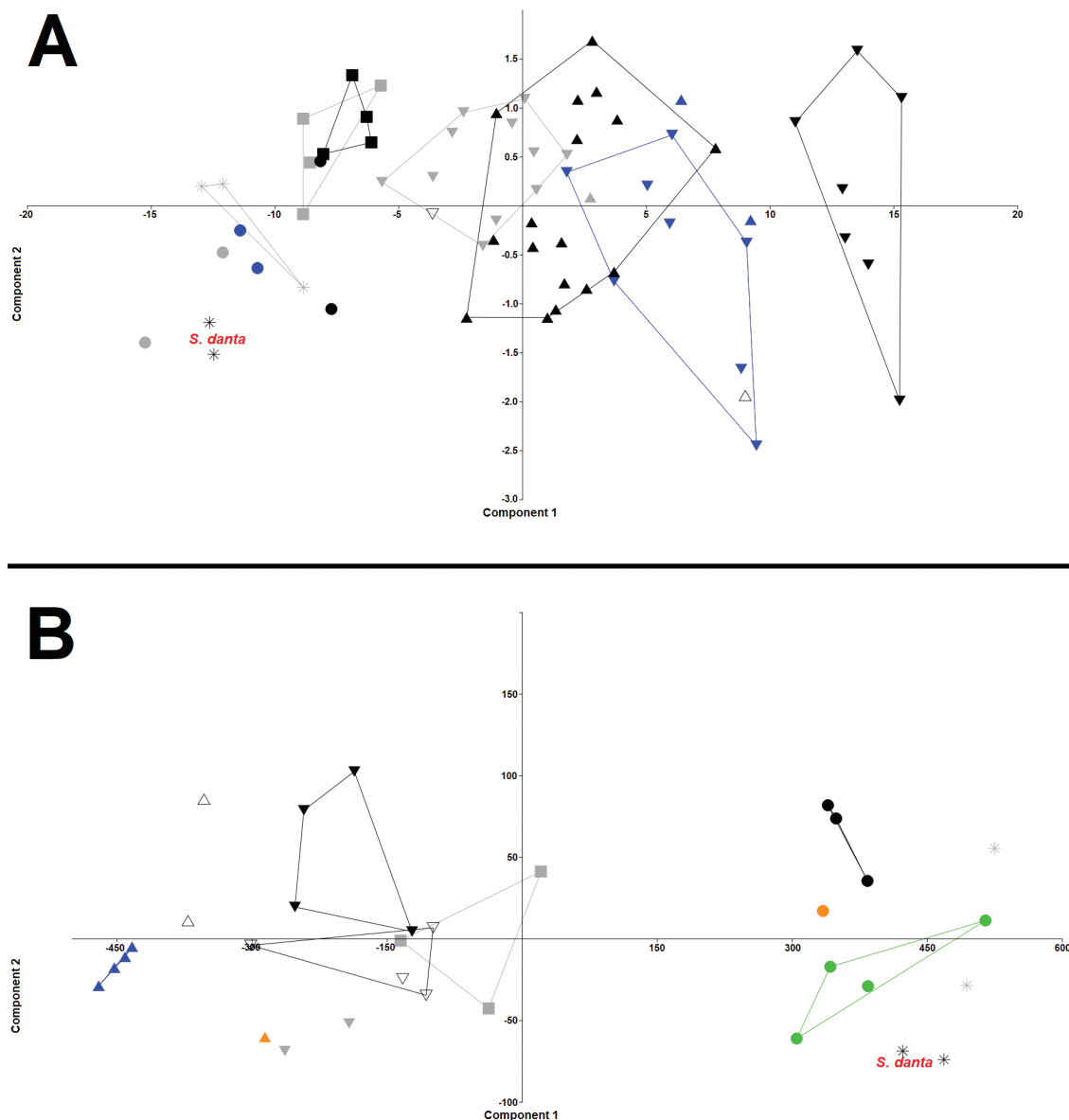


Figure 3. Plots of PCA of **A.** Morphometric characteristics (males and females) and **B.** Acoustic variables showing the position of *Synapturanus danta* sp. nov. (black asterisk) from unnamed lineages of Fouquet et al. (2021a): *Synapturanus* sp. “Juami” (gray squares); *S.* sp. “Iça1” (black squares only females); *S.* cf. *mirandariberoi* (black triangles); *S.* sp. “Purus” (blue triangles); *S.* sp. “Taboca” (gray triangle); *S.* sp. “Tapajos” (white triangle); *S. zombie* (inv. black triangle); *S. mesomorphus* (inv. gray triangle); *S. ajuricaba* (inv. blue triangle); *S.* sp. “Neblina” (inv. white triangle); *S.* sp. “Divisor” (gray asterisk); *S.* sp. “Ecuador” (black dot); *S.* sp. “Venezuela” (gray dot); *S.* sp. “Iça2” (blue dot); *S. rabus* (orange dot), *S.* sp. “Nanay” (green dots).

the new species is nested within the Western clade of Fouquet et al. (2021a) along with *S. rabus* Pyburn 1977, the only nominal species of this clade, and four other terminals belonging to candidate species. Within the Western clade, only the node clustering the new species and its sister putative species (MZUSP 159223, an undescribed taxon from Serra do Divisor, Acre, Brazil) has strong support (bootstrap value of 100). The close relationships between the new species and the four other terminals in the Western clade are supported by 16S rRNA genetic distances (Figshare <https://doi.org/10.6084/m9.figshare.17702231>), which is smallest for the pairwise comparison with the Sierra do Divisor specimen (2.8%), and < 9% for the comparisons with the other three species (range 7.6–8.9%).

PCA analysis

The PCA plots (Fig. 3A–B) show a clustering similar as those obtained by Fouquet et al. (2021a). The new species from Peru is morphologically most similar to undescribed taxa: *Synapturanus* sp. “Divisor”, *S.* sp. “Venezuela”, *S.* sp. “Iça 2” and *S.* sp. “Ecuador” (Fig. 3A), all belonging to the Western clade sensu Fouquet et al. (2021a). Frog size influenced the PCA, because the plots of size-independent PCA did not show a clear clustering of species according to phylogeny or geography (Suppl. material 2, 3). The size-uncorrected PCA showed a clear clustering that agreed with phylogenetic groupings and the geographic distribution of species. The first component of the PCA of morphometric size-dependent analyses explained more than 96% of the

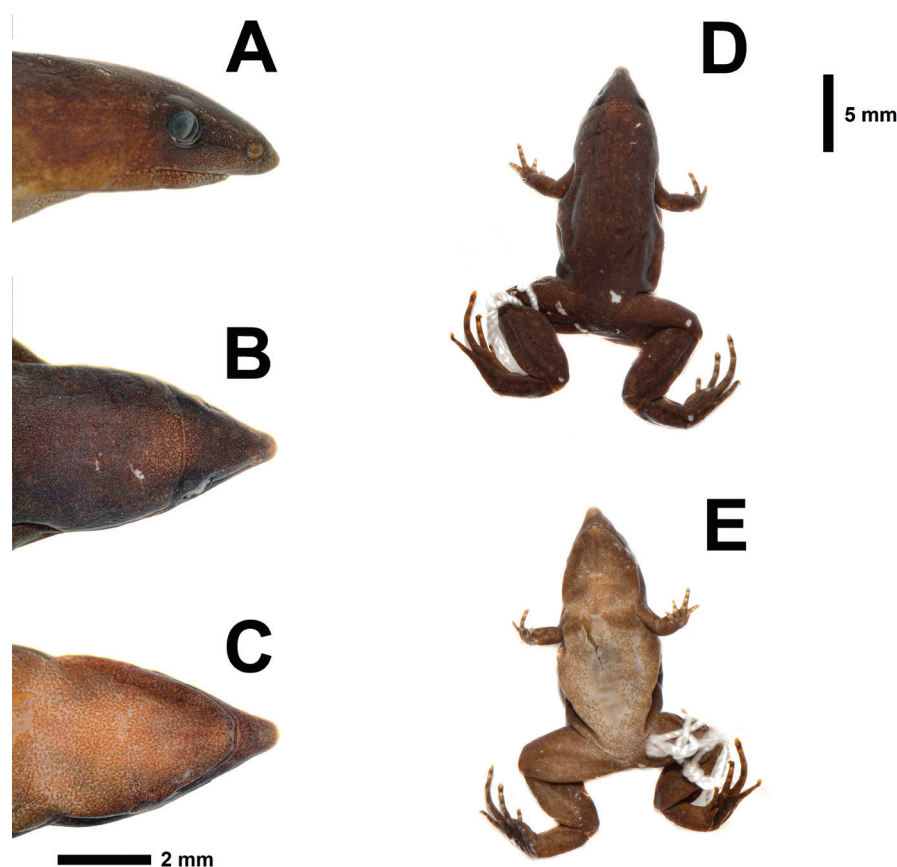


Figure 4. Lateral (A.), dorsal (B.) and ventral (C.) views of the head; Dorsal (D.) and ventral (E.) views of the body of the holotype (CORBIDI 21050, SVL=17.9 mm) of *Synapturanus danta* sp. nov. Photographs by Eduardo Quispe-Salcedo.

variance, while the first PC of the size-corrected PCA explained just 45% of the variance (Suppl. material 2: Appendix 2). There seems to be no effect of frog sex, and individuals of both sexes clustered together with males of their species more than they were to other species. Using the same criteria as used by Fouquet et al. (2021a), we relied on the extent of overlapping in the morphospace of our PCAs to inform species delimitations. The morphospace of the new species did not overlap with that of any other species.

Plot of PCA analyses of the three acoustic variables resulted in clustering of species of the Western clade (*Synapturanus* sp. “Divisor”, *S.* sp. “Nanay”, *S.* sp. “Ecuador”, *S. rabus* and the new species described herein Fig. 3B). The first PC of the analysis of acoustic variables explained 97% of the variance. The “bioacoustics space” of the new species did not overlap with any of its congeners of the Western clade (Fig. 3B), similar to the lack of overlapping of morphospace on PCA plots of morphometric data (Fig. 3A).

***Synapturanus danta* sp. nov.**

<http://zoobank.org/C55B4D25-62C8-42C2-8AA0-501F9086BC02>

Synapturanus sp. (Chávez et al. 2021)

Holotype. Male CORBIDI 21050 (Figs. 4A–E, 5A, B), collected by Michelle E. Thompson, David Sánchez, and Germán Chávez at Campamento Quebrada Federico

(02°31'34.7"S, 70°39'17.2"W; 110 m a.s.l.), Putumayo Province, Loreto Department, Peru, on 7 November 2019.

Paratopotypes. Juvenile CORBIDI 21013 (Fig. 5E, F), collected by Michelle E. Thompson, David Sánchez, and Germán Chávez at the same site on 6 November 2019; male CORBIDI 21051 (Fig. 5C, D), same data as holotype.

Definition and diagnosis. (1) A small-sized *Synapturanus* (SVL of 17.6–17.9 mm in adult males, females unknown); (2) head dorsally flat in lateral view; (3) eyes small, slightly larger than half the size of the eye-naris distance; (4) fingertips tapering without discs; (5) subarticular tubercles not visible on fingers; (6) thenar tubercle indistinct, palmar tubercle distinct; (7) fingers with preaxial and postaxial fringes (except preaxially on Finger IV), strongly visible on Fingers II and III pre and post axially; (8) toe tips slightly expanded in toes II and III; (9) inner metatarsal tubercle indistinct, outer metatarsal tubercle indistinct; (10) dorsal color pattern chocolate brown without spots or blotches, a stripe along the canthus rostralis and upper eyelid only present in juveniles; (11) throat and ventral surface of limbs cinnamon brown or pinkish brown, chest and belly cyan white; (12) call consisting of a tonal note 0.054–0.063 seconds in length with a slight downward frequency modulation (delta 0–94 Hz) and a dominant frequency at 1.73–1.81 kHz (Table 3).

Table 1 summarizes morphological differences between the new species and the current described congeners. In appearance, *Synapturanus danta* sp. nov. is easily

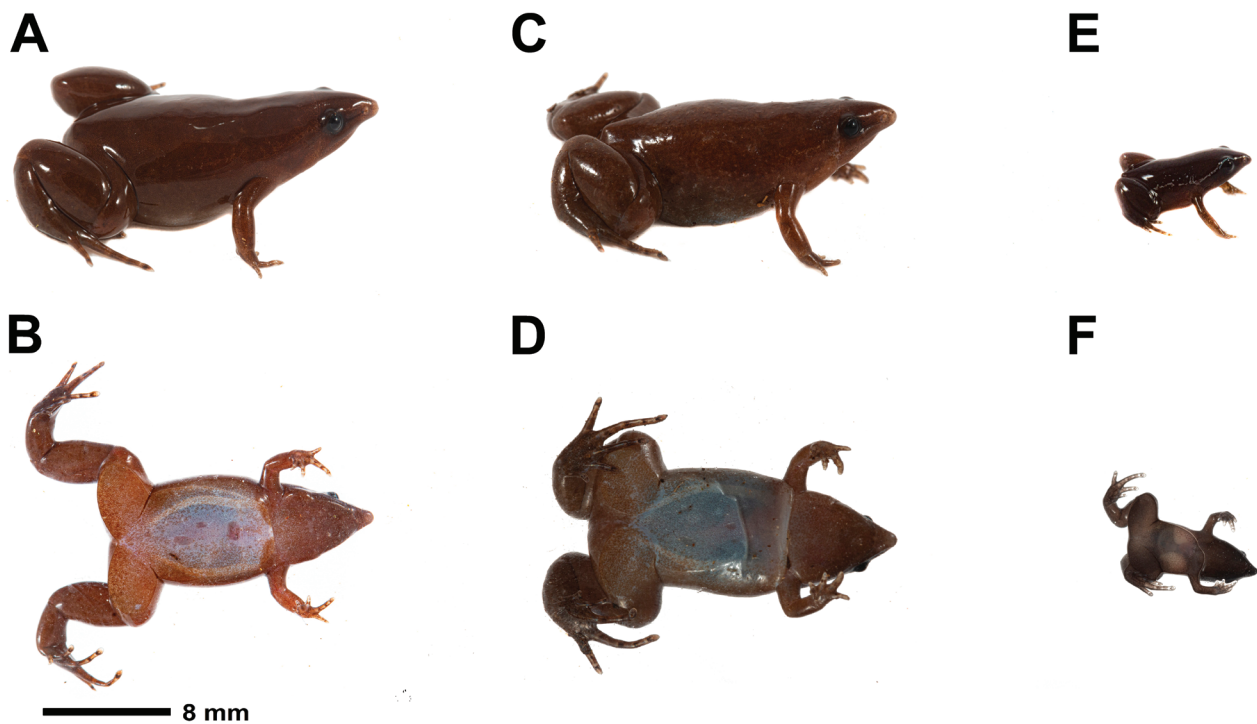


Figure 5. Type series of *Synapturanus danta* sp. nov. in life. **A, B.** Dorsal and ventral view of male CORBIDI 21050 (holotype, SVL=17.9 mm); **C, D.** Dorsal and ventral view of male CORBIDI 21051 (SVL=17.6 mm); **E, F.** Dorsal and ventral view of male CORBIDI 21013 (SVL=7.5 mm). Photographs by Germán Chávez.

distinguishable from most of its congeners, except for *S. rabus* and *S. salseri*, by bearing a flat head in lateral view (vs convex in the rest of species). The new species can be further distinguished from *S. rabus* (data for *S. rabus* taken from Pyburn 1977 and Fouquet et al. 2021b) by having an indistinct tympanum (vs visible), an eye slightly larger than half of the size than eye-naris distance (vs slightly smaller than half of the size of eye-naris distance), lacking canthal stripe in adults (vs present), and an advertisement call with a note length of 0.054–0.063 seconds (vs 0.03 seconds). From *S. salseri*, by being smaller with a mean SVL of 17.8 mm in adult males (vs 26.4 mm), and by having a visible palmar tubercle (vs absent), no metacarpal and inner metatarsal tubercles (vs present), no spots or stripes on dorsal surface of body (vs orange or gray spots and a discontinuous canthal stripe present), and by having an advertisement call with a dominant frequency ranging from 1.73–1.81 kHz (vs 1.10–1.47 kHz in *S. salseri*). Furthermore, the new species can be differentiated from *S. ajuricaba* by having a non-visible tympanum (vs visible), eyes being slightly larger than half the eye-naris distance (vs slightly smaller than half the eye-naris distance), an advertisement call with a dominant frequency of 1.73–1.81 kHz (vs 1.01–1.12 kHz); and by lacking spots on dorsum (vs present). Moreover, the new species is differentiable from *S. mesomorphus*, *S. mirandariberoi* and *S. zombie* by having a slender body shape (vs robust in *S. mirandariberoi* and *S. zombie*), non-rounded fingers (vs rounded in *S. mesomorphus* and *S. mirandariberoi* and having a rounded disc on fourth finger in *S. zombie*), a palmar tubercle present (vs absent), lacking thenar and metatarsal tubercle (vs present), having an advertisement call with a higher dominant frequency, ranging from 1.73

kHz to 1.81 kHz (vs 1.06–1.13 kHz in *S. mesomorphus*, 1.10–1.47 kHz in *S. mirandariberoi*, and 1.06–1.19 kHz in *S. zombie*), and by lacking spots or speckles on dorsum (vs present). Additionally, the new species differs from a genetically related undescribed species (Fig. 2) from Serra do Divisor National Park, western Brazil (*Synapturanus* sp. “Divisor” voucher number MZUSP 159223, Fouquet et al. 2021a), by having a longer head which is in average 27% of the SVL, $n=3$ (vs 19%, $n=3$), a shorter nose being 33% of the head length, $n=3$ (vs 47%, $n=3$) and shorter tibia which is about 32% of the SVL, $n=3$ (vs 40%, $n=3$).

Description of the holotype. An adult male (CORBIDI 21050), 17.9 mm SVL; body stout; head slightly wider than long, HL 24% of SVL; dorsal and ventral skin smooth from head to cloaca; linea masculina visible through the translucent ventral skin in life, extending ventrolaterally from axilla to groin; supratympanic fold barely visible, running from the posterior corner of the eye to the level of the neck; snout long and strongly protruding, projecting way beyond the end of the lower jaw (1.34 mm), tip of the nose protruding, rounded in dorsal and lateral view. Eyes small, 66% of EN; nares located laterally, closer to the tip of the snout (0.69 mm) than to the eye (1.51 mm); canthus rostralis acutely rounded, loreal region strongly concave, grooved; IN 19% of HW; EN 35% of HL. Tympanum barely visible; choanae small (less than 50% of ED), oval, located anterolaterally, no odontophores. Forelimb robust, skin smooth; HAND 15% of SVL; Finger II longer than Finger I when fingers adpressed; fingers short, tips tapering excepting Finger III, unwebbed, with pre- and postaxial fringes, particularly developed on Fingers II and III where fringes extend towards the base

of fingers; no finger discs; relative length of adressed fingers III > IV > II > I; subarticular tubercles not visible on fingers; thenar tubercle indistinct, palmar tubercle small, oval. Glandular unpigmented supracarpal pad present. Hind limb robust, skin smooth; TL 28% of SVL; FL 41% of SVL; relative length of adressed toes IV > III > V > II > I; toes without discs, tapering on I, IV, and V, expanded on II and II. Toes unwebbed with narrow pre- and postaxial fringes. Subarticular tubercles not visible on toes; inner metatarsal tubercle indistinct, outer metatarsal tubercle indistinct. Metatarsal fold absent.

Color of holotype in life. Dorsum and flanks chocolate brown without spots. Absence of a stripe along the canthus rostralis and upper eyelid. Snout white, unpigmented. Throat cinnamon brown with scattered pale orange or yellow dots; chest and belly translucent cyan with white small melanophores (Fig. 4A, B). Upper and lower arm and dorsal surfaces of thigh, shank and tarsus similar to the dorsum in color. Glandular supracarpal pad translucent white.

Color of holotype in preservative. Dorsum dark brown, nose sulphur yellow. Throat creamy yellow with brown speckles. Chest and belly creamy yellow, with brown speckles toward the flanks, ventral surfaces of limbs yellowish brown. (Fig. 4A–E).

Variation. For morphometric variation see Table 2. Sexual dimorphism unknown. A cyan-white discontinuous canthal stripe extending to the upper eyelid and then, reaching the groins is present in juvenile CORBIDI 21013 (Fig. 5E, F). Dorsal coloration of this juvenile is dark brown with tiny pale orange dots on dorsal surface of limbs. Ventral cyan-white coloration reaching the edge with the flank in male CORBIDI 21051. Ventral surface of feet black in male CORBIDI 21051 (Fig. 5C, D).

Advertisement call. *Synapturanus danta* sp. nov. (n=2) emits single tonal notes (mean note length 0.059, range 0.054–0.063 seconds, SD=0.003) every 4.083 seconds on average (inter-note range 3.777–4.552 seconds, SD=0.300). The dominant frequency is 1.763 kHz on average (range 1.734–1.809 kHz, SD=0.031) with a slight downward modulation (mean 0.059, range 0.000–0.094 kHz, SD=0.049); a harmonic structure is present (Fig. 6, Table 3).

Etymology. The specific epithet is a noun in apposition and refers to the Amazon Tapir (*Tapirus terrestris*), a large mammal locally known as “Danta”. During our expedition, the first time that local people and other researchers in the team spotted one of these frogs, they called it “Rana Danta”, because its head profile reminded them of the head of the Amazon Tapir.

Distribution, habitat and natural history. *Synapturanus danta* sp. nov. is only known from a population in the Lower Putumayo River Basin, Loreto, Peru (Fig. 1). All individuals were captured at night in galleries underneath roots of *Clusia* spp. in habitats classified as Amazon Peatlands (Xu et al. 2018; Figs 1, 7), at the beginning of the rainy season. This peatland ecosystem is thought to occur over large areas in the Putumayo Basin (Figs 1, 7; Gumbrecht et al. 2017, Xu et al. 2018.); however, some of the areas predicted to be peatlands have yet to be

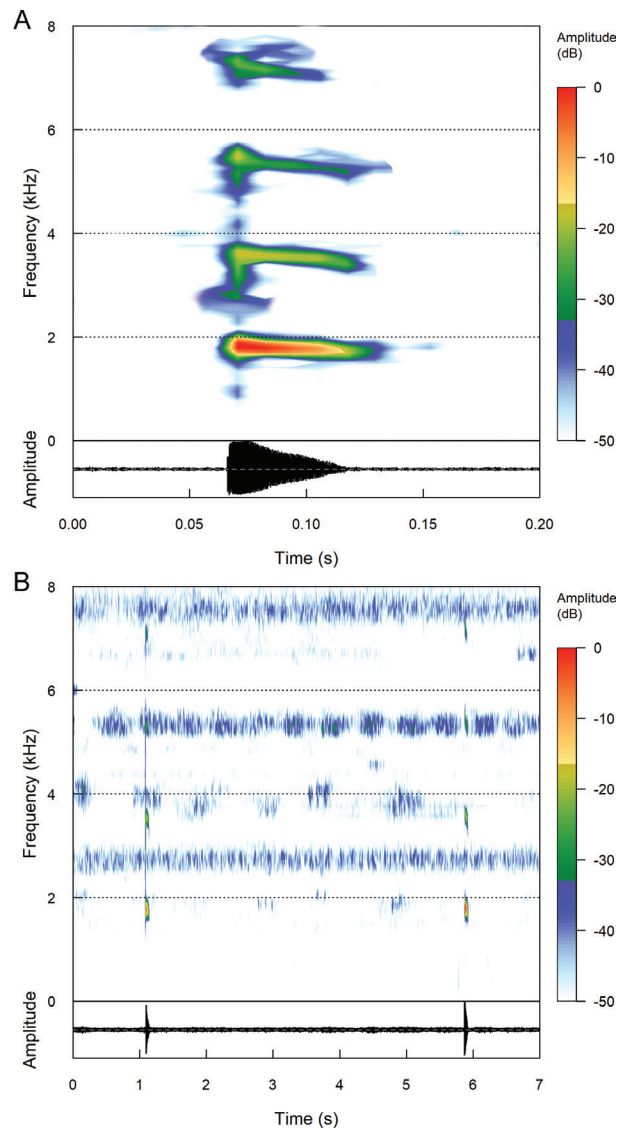


Figure 6. Audio spectrograms and oscillograms of the advertisement call of the holotype (CORBIDI 21050) of *Synapturanus danta* sp. nov., recorded at night, in the Lower Putumayo River basin. **A.** Single call; **B.** Series of two calls

validated with field surveys. *Synapturanus danta* sp. nov. inhabits the soils of stunted pole forests growing on peat. The vegetation at the type locality consists of treelet species which are common in stunted varillal and chamizal forests on white sand in Loreto, Perú (e.g., *Mauritiella armata*, *Macrolobium limbatum*, *Retiniphyllum concolor*, *Dendropanax resinous*, *Remijia ulei*, as well as the filmy ferns in the genus *Trichomanes*), treelet species only known to grow in Loreto in stunted forests on peat soils (e.g., *Tabebuia insignis* var. *monophylla*, *Diploptropis purpurea*, *Graffenrieda limbata*, *Macrolobium* sp., *Rapatea ulei*) and small populations of other common wetland species such as *Mauritia flexuosa* and *Euterpe precatoria* (Ríos Paredes et al. 2021). These peatlands are seasonally saturated ecosystems, with periods of high-water levels resulting in a matrix of pools formed by rainwater and unsaturated land sitting above the pooled water, and periods of drying down of the landscape when there is low to no rainfall.



Figure 7. Panoramic view of the type locality (A.) and a view of the landscape in the Amazonian Peatlands inhabited by *Synapturanus danta* sp. nov. (B.). Photographs by Alvaro del Campo (A.) and Luis Montenegro (B.).

We sampled during a period of rising water levels at the beginning of the rainy season; however, many unsaturated areas were present, scattered throughout the habitat around root chambers of individual trees and palms. Adult males were caught in those unsaturated areas within chambers and galleries of 15–30 cm depth, underneath roots of *Clusia* spp. Instead, the only juvenile collected (CORBIDI 21013) was captured only 5 cm depth, jumping between roots of the same species of tree where the adults were calling from. All individuals were observed 3–4 meters apart from each other.

Discussion

Previous research has demonstrated that *Synapturanus* diversity is widely underestimated (Fouquet et al. 2021a) and taxonomic gaps have started to be filled only recently in inventories of poorly sampled localities. Fouquet et al. (2021b) described three new species and identified another fifteen candidate species (Fouquet et al. 2021a). One of the likely reasons for the poor taxonomical knowledge in *Synapturanus* is their fossorial habit, which has resulted in scarcity of specimens in collections, preventing scientists from gathering enough evidence to perform integrative studies on the genus. Here, as recommended by Fouquet et al. (2021a), we apply an integrative approach to support our description, increasing the ability to compare material in museums with other taxa by using the same data recorded. Thus, genetic, acoustic as well as morphological features concluded that our specimens belong to a new species and gave us enough confidence to describe *Synapturanus danta* as a separate taxon.

Although *S. danta* sp. nov. is the sister species of an undescribed lineage from Sierra del Divisor (*Synapturanus* sp. “Divisor”, Fig. 2), morphological differences (described in diagnosis section) and acoustic features (Fig. 3B) led us to consider *S. danta* sp. nov. as a distinct species.

Also, the new species lives relatively close to the lineages “Iça 1” and “Iça 2” proposed by Fouquet et al. (2021a), North and South of the Putumayo River respectively, and around 300 km airline distance (Fig. 1). Fouquet et al. (2021a) suggested that the fossorial habits of *Synapturanus* frogs are linked to the body shape and proposed three phenotypes to explain this hypothesis. Based on this, *S. danta* sp. nov. fits the “phenotype 1” whereas *Synapturanus* sp. “Iça 1” corresponds to “phenotype 2”. Likewise, our PCA analyses (Fig. 3A, B) shows that *S. danta* sp. nov. differs morphologically from its described congeners as well as from the unnamed delimited lineages (Fig. 3A), among them, *Synapturanus* sp. “Iça 2”. In general, it shares some similarities with species of the Western clade (*S.* sp. “Venezuela”, *S.* sp. “Divisor”, *S.* sp. “Iça 2” and *S.* sp. “Ecuador”) and the Central clade (*S.* sp. “juami” and *S.* sp. “Iça 1”) as they cluster together along the first PC on the PCA plot, as opposed to those of the Eastern clade (Fig. 3A).

Regarding the phenotype and its relationship to fossoriality, we found that *S. danta* sp. nov. lives underground in shallow galleries under the loose, wet and soft soil that covers the ground of the Amazon Peatlands of the Putumayo River Basin. Subsequently, digging galleries in these soils may present minimal mechanical challenges and likely does not require a robust body shape (as seen in the phenotype 1 of Fouquet et al. 2021a). Thus, our data leads us to support the hypothesis proposed by Fouquet et al. (2021a, b) that phenotype 1 populations inhabiting western Amazonia are less fossorial than those of phenotype 2 or 3 from central and eastern Amazonia and the Guiana shield. However, this remains speculative and needs to be tested in further research.

Currently, there is minimal deforestation affecting the peatlands around the type locality (Jarrett et al. 2021). Given that only three specimens are known, there is large uncertainty in the distribution and population status of this species. Therefore, we suggest the IUCN Red List category of Data Deficient.

Acknowledgements

We thank Antoine Fouquet for his value feedback which helped us to improve this article. This research would not have been possible without the valuable help of the local people from the Comunidad Nativa Tres Esquinas who kindly and patiently guided us deep into the forest to find the new species. The fieldwork was funded by the generous support of an anonymous donor and additionally by Bobolink Foundation, Connie and Dennis Keller, Mike and Lindy Keiser, Gordon and Betty Moore Foundation, and the Field Museum. We thank Corine Vriesendorp and Alvaro del Campo for trusting our work. We also appreciate the help of Marcos Rios and Luis Montenegro with the identification of the plants in the type locality of the new species. GC is deeply grateful with The Cornell Ornithology Lab by providing the acoustic equipment that made possible the call recordings for this research. DAS was supported by Instituto Amazónico de Investigaciones Científicas SINCHI in Colombia, and a post-doctoral fellowships funded by Instituto Colombiano para el Desarrollo de la Ciencia y la Tecnología “Francisco José de Caldas” -Colciencias.

References

- Anderson EP, Jenkins CN, Heilpern S, Maldonado-Ocampo JA, Carvajal-Vallejos FM, Encalada AC, Rivadeneira JF, Hidalgo M, Cañas CM, Ortega H, Salcedo N, Maldonado M, Tedesco PA (2018) Fragmentation of Andes-to-Amazon connectivity by hydropower dams. *Science Advances* 4: eaao1642. <https://doi.org/10.1126/sciadv.aao1642>
- Araya-Salas M, Smith-Vidaurre G (2017) warbleR: an R package to streamline analysis of animal acoustic signals. *Methods in Ecology and Evolution* 8: 184–191. <https://doi.org/10.1111/2041-210X.12624>

- Chávez G, Sánchez DA, Thompson ME (2021) Anfibios y reptiles/ Amphibians and reptiles. In: Jarrett CC, Thompson ME, Pitman N, Vriesendorp CF, Reyes D, Lemos AA, Carrasco-Rueda F, Matapi Yucuna W, Salazar Molano A, Sáenz Rodríguez AR, Ferreyra F, del Campo A, Morales M, Alfonso A, Torres Tuesta T, Herrera Vargas MC, García Ortega C, Cardona Uribe V, Kotlinski N, Moskovits DK, de Souza LS, Stotz DF (Eds) Colombia, Perú: Bajo Putumayo-Yaguas-Cotuhé. Rapid Biological and Social Inventories Report 31. Field Museum, Chicago, 145–156, 393–403, 574–581.
- Fouquet A, Gilles A, Vences M, Marty C, Blanc M, Gemmell NJ (2007) Underestimation of species richness in Neotropical frogs revealed by mtDNA analyses. *PLoS ONE* 2: e1109. <https://doi.org/10.1371/journal.pone.0001109>
- Fouquet A, Leblanc K, Fabre A, Rodrigues MT, Menin M, Courtois EA, Dewynter M, Hölting M, Ernst R, Peloso P, Kok PJR (2021a) Comparative osteology of the fossorial frogs of the genus *Synapturanus* (Anura, Microhylidae) with the description of three new species from the Eastern Guiana Shield. *Zoologischer Anzeiger* 293: 46–73. <https://doi.org/10.1016/j.jcz.2021.05.003>
- Fouquet A, Leblanc K, Framit M, Réjau A, Rodrigues MT, Castroviejo-Fisher S, Peloso PLV, Prates I, Manzi S, Suescun U, Baroni S, Moraes LJCL, Recoder R, de Souza SM, Dal Vecchio F, Camacho A, Ghellere JM, Rojas-Runjaic FJM, Gagliardi-Urrutia G, de Carvalho VT, Gordo M, Menin M, Kok PJR, Hrbek T, Werneck FP, Crawford AJ, Ron SR, Mueses-Cisneros JJ, Rojas Zamora RR, Pavan D, Simões PI, Ernst R, Fabre A-C, Species diversity and biogeography of an ancient frog clade from the Guiana Shield (Anura: Microhylidae: *Adelastes*, *Otophryne*, *Synapturanus*) exhibiting spectacular phenotypic diversification. *Biological Journal of the Linnean Society* 132: 233–256. <https://doi.org/10.1093/biolinnean/blaa204>
- Gumbrecht T, Roman-Cuesta RM, Verchot L, Herold M, Wittmann F, Householder E, Herold N, Murdiyarto (2017) An expert system model for mapping tropical wetlands and peatlands reveals South America as the largest contributor. *Global Change Biology* 23: 3581–3599. <https://doi.org/10.1111/gcb.13689>
- Hammer Ø, Harper DAT, Ryan PD (2001) Past: Paleontological Statistics Software Package for Education and Data Analysis. *Palaeontologia Electronica* 4: 1–9.
- Jarrett CC, Thompson ME, Pitman N, Vriesendorp CF, Reyes D, Lemos AA, Carrasco-Rueda F, Matapi Yucuna W, Salazar Molano A, Sáenz Rodríguez AR, Ferreyra F, del Campo A, Morales M, Alfonso A, Torres Tuesta T, Herrera Vargas MC, García Ortega C, Cardona Uribe V, Kotlinski N, Moskovits DK, de Souza LS Stotz DF (Eds) (2021) Colombia, Perú: Bajo Putumayo-Yaguas-Cotuhé. Rapid Biological and Social Inventories Report 31. Field Museum, Chicago, 618 pp.
- Katoh K, Standley DM (2013) MAFFT multiple sequence alignment software version 7: improvements in performance and usability. *Molecular Biology and Evolution* 30: 772–780. <https://doi.org/10.1093/molbev/mst010>
- Köhler J, Jansen M, Rodríguez A, Kok PJR, Toledo LF, Emmrich M, Glaw F, Haddad CFB, Rödel MO, Vences M (2017) The use of bioacoustics in anuran taxonomy: theory, terminology, methods and recommendations for best practice. *Zootaxa* 4251(1): 1–124. <https://doi.org/10.11646/zootaxa.4251.1.1>
- Nguyen LT, Schmidt HA, von Haeseler A, Minh BQ (2015) IQ-TREE: A fast and effective stochastic algorithm for estimating maximum-likelihood phylogenies. *Molecular biology and evolution* 32: 268–274. <https://doi.org/10.1093/molbev/msu300>
- Pitman NCA, Vriesendorp CF, Alvira Reyes D, Moskovits DK, Kotlinski N, Smith RC, Thompson ME, Wali A, Benavides Matarazzo M, del Campo A, Rivera González DE, Rivera Chávez L, Rosenthal AD, Álvarez Alonso J, Díaz Ñaupari ME, de Souza LS, Ferreyra Vela FR, Gonzales Tanchiva CN, Jarrett CC, Lemos AA, Sáenz Rodríguez AR, Stotz DF, Suwa T, Pariona Fonseca M, Ravikumar A, Torres Tuesta T, Bravo A, Catenazzi A, Díaz Alván J, Gagliardi-Urrutia G, García-Villacorta R, Hidalgo MH, Mori Vargas T, Mueses-Cisneros JJ, Núñez-Iturri G, Pequeño I, Ríos Paredes MA, Rodríguez LO, Stallard RF, Torres Montenegro LA, Venegas PJ, von May R, Barbagelata Ramírez N, Maldonado Ocampo JA, Mesones Acuy I (2021) Applied science facilitates the large-scale expansion of protected areas in an Amazonian hot spot. *Science Advances* 7: eabe2998. <https://doi.org/10.1126/sciadv.abe2998>
- R Core Team (2021) R: A language and environment for statistical computing. R Foundation for Statistical Computing, Vienna, Austria. <https://www.R-project.org/>
- Ríos Paredes MA, Acosta Arango JD, Rodríguez Duque WD, Torres Montenegro LA, Vriesendorp CF (2021) Vegetación/Vegetation. In: Jarrett CC, Thompson ME, Pitman N, Vriesendorp CF, Reyes D, Lemos AA, Carrasco-Rueda F, Matapi Yucuna W, Salazar Molano A, Sáenz Rodríguez AR, Ferreyra F, del Campo A, Morales M, Alfonso A, Torres Tuesta T, Herrera Vargas MC, García Ortega C, Cardona Uribe V, Kotlinski N, Moskovits DK, de Souza LS, Stotz DF (Eds) Colombia, Perú: Bajo Putumayo-Yaguas-Cotuhé. Rapid Biological and Social Inventories Report 31. Field Museum, Chicago, 124–130, 374–378.
- Sueur J, Aubin T, Simonis C (2008) Seewave: a free modular tool for sound analysis and synthesis. *Bioacoustics* 18: 213–226. <https://doi.org/10.1080/09524622.2008.9753600>
- Xu J, Morris PJ, Liu J, Holden J (2018) PEATMAP: Refining estimates of global peatland distribution based on a meta-analysis. *Catena* 160: 134–140. <https://doi.org/10.1016/j.catena.2017.09.010>
- Ziesler R, Ardizzone GD (1979) Inland waters of Latin America. Organización de las Naciones Unidas para la Agricultura y la Alimentación. Procedencia del original, Universidad de Texas, 171 pp.

Supplementary material 1

Appendix 1

Authors: Germán Chávez, Michelle E. Thompson, David A. Sánchez, Juan Carlos Chávez-Arribasplata, Alessandro Catenazzi

Data type: Text file

Explanation note: GenBank accession numbers for the taxa and genes sampled in this study.

Copyright notice: This dataset is made available under the Open Database License (<http://opendatacommons.org/licenses/odbl/1.0>). The Open Database License (ODbL) is a license agreement intended to allow users to freely share, modify, and use this Dataset while maintaining this same freedom for others, provided that the original source and author(s) are credited.

Link: <https://doi.org/10.3897/evolsyst.6.80281.suppl1>

Supplementary material 2

Appendix 2

Authors: Germán Chávez, Michelle E. Thompson, David A. Sánchez, Juan Carlos Chávez-Arribasplata, Alessandro Catenazzi

Data type: Text file

Explanation note: Values of percentage of variance of each PC on the PCA analyses performed in this study.

Copyright notice: This dataset is made available under the Open Database License (<http://opendatacommons.org/licenses/odbl/1.0>). The Open Database License (ODbL) is a license agreement intended to allow users to freely share, modify, and use this Dataset while maintaining this same freedom for others, provided that the original source and author(s) are credited.

Link: <https://doi.org/10.3897/evolsyst.6.80281.suppl2>

Supplementary material 3

Supplementary File 1

Authors: Germán Chávez, Michelle E. Thompson, David A. Sánchez, Juan Carlos Chávez-Arribasplata, Alessandro Catenazzi

Data type: COL

Explanation note: PCA plots of size-independent morphometric measurements, made with residuals of regressions of measurements with SVL as a proxy of size, of males and females provided in Fouquet et al. (2012a) and *Synapturanus danta* sp. nov. A) PC 1 vs PC2; B) PC1 vs PC3. Percentages of variance for each PC are provided in Appendix 2.

Copyright notice: This dataset is made available under the Open Database License (<http://opendatacommons.org/licenses/odbl/1.0>). The Open Database License (ODbL) is a license agreement intended to allow users to freely share, modify, and use this Dataset while maintaining this same freedom for others, provided that the original source and author(s) are credited.

Link: <https://doi.org/10.3897/evolsyst.6.80281.suppl3>